

Power Quality Control Center for the Microgrid System

Y.H. Chung*, H.J. Kim*, K.S. Kim*, J.W. Choe* and Jaeho Choi**

* LS Industrial Systems Co. Ltd / R&D Center, Anyang, Korea. Email: yhchung@lisis.biz

** ChungBuk National University, Cheongju, Korea. Email: choi@chungbuk.ac.kr

Abstract— This paper describes the power quality control center (PQCC) for the microgrid systems composed of the photovoltaic power, wind power, fuel cell power, gas engine generator and various power quality loads. PQCC is consisted of a series voltage compensator and a parallel battery energy storage system (BESS). The series voltage compensator is composed of high performance DVR (Dynamic Voltage Restorer) with the neural network controlled voltage disturbance detector and the real-time output voltage regulator. DVR supplies the high quality power to the premium quality load by compensating the voltage disturbance such as voltage sag.

On the other hand, BESS was employed to make the microgrid voltage to be stable during the isolation mode operation while to compensate the harmonic current of load and to reduce the peak load during the grid-connected mode. During the isolation mode operation, BESS can quickly respond to the sudden changes in both demand and supply of electricity that gas engine can't copy with. In addition, BESS is for the stabilization of power fluctuation caused by the uncontrollable power source such as the photovoltaic power and the wind power. During grid-connected mode operation, BESS is operated as APF (Active Power Filter) with the function of battery charger.

In this paper, the overall operations of the microgrid systems are described and the detailed descriptions and control for PQCC are given with the computer simulations. Finally, conclusions are given.

Keywords— Microgrid, BESS, DVR, Power Quality

I. INTRODUCTION

In recent years, in Europe, microgrid is entering its third major round under the 7th European Commission Framework Program; in the U.S., one specific microgrid concept is undergoing rigorous laboratory testing, and in Japan, four major publicly sponsored and two privately sponsored demonstrations are in progress; in Korea, ten power information technology based national projects are in progress, and one of them is the development of

critical elements for microgrid system and the construction of microgrid demonstration site. [1-2].

Microgrid is grouping of the generating sources and loads operating semi-independently from the main grid, typically interconnected at a single point of common coupling (PCC). The microgrid may include gas engine generator, fuel cells, photovoltaic generation or other small scale renewable sources, electrical and heat storage devices and controllable end-user loads. Integrating total power ratings of microgrid system is typically less than 1MW with peak electrical loads of less than about 2MW. Depending on the main concerns, the object of microgrid system is different from each other in the developed countries. The most likely features of the microgrid system are as follows:

- 1) Efficient meeting total system energy requirement, often by including combined heat and power (CHP) technology, especially for building heating and/or cooling.
- 2) Providing heterogeneous levels of electricity security, quality, reliability and availability (SQRA) that match the requirement of end users.
- 3) Appearing to the main grid as controlled entity, akin to a current local utility customer, or conversely akin to a small embedded generation source if the microgrid exports.

Reviewing all kinds of microgrid system, we can find that two kinds of energy storage systems are essential for the optimal use of energy or the balance of energy supply and demand. One of them is electrical energy storage system such as BESS while the other one is the heat energy storage system. Even though the electrical energy and the heat energy are closely combined, in this paper, our main concerns will be confined to the electrical energy storage with the power quality problems in microgrid system. For the power quality enhancement, we adopted the PQCC composed of DVR and BESS with a common use of battery to minimize the system cost.

First, the essential parts of DVR are how to detect the voltage disturbance and how to compensate it as fast as possible respectively. In general the most voltage sag is owing to the single phase ground fault. This means that the typical voltage waveforms are unbalanced when the voltage sag occurs. In this paper, we proposed a new

voltage disturbance detection method with neural network control. Through the proposed method we can track the amplitude of each phase voltage independently and instantaneously. As a result, it is possible to minimize the time delay to determine the instance of voltage disturbance even under the severe unbalanced voltage conditions.

Second, the line voltages are typically unbalanced under the typical voltage sag condition. In that case, we need to inject a zero sequence voltage to the utility line. Namely we need three single phase inverters and a five-leg transformer so that we can inject a zero phase sequence voltage. This implies that we need a new voltage control regulator for single phase inverter to compensate the unbalanced voltage disturbance. We proposed a new modified d-q transformed voltage regulator for single phase inverter to obtain the fast dynamic response and the robustness, where three independent single phase inverters are controlled by using the source voltage amplitude obtained by neural network controller.

Third, the control of BESS is similar to the conventional PWM converter except for the additional battery charger. Depending on the operating mode of microgrid, BESS can be regarded as UPS, APF, the load managing device, the power balancing device and the voltage stabilizer. In this paper, BESS is confined to the function of APF with the battery charger. Charging and discharging command for the BESS will come from the high level energy management system (EMS) that schedules the operations of the controllable power source such as the gas engine, fuel cell and the BESS.

In this paper, the overall operations of the microgrid systems with PQCC are described, and the detailed controls for PQCC are given with the computer simulations. Finally, conclusions are given.

II. DESCRIPTIONS OF MICROGRID AND PQCC

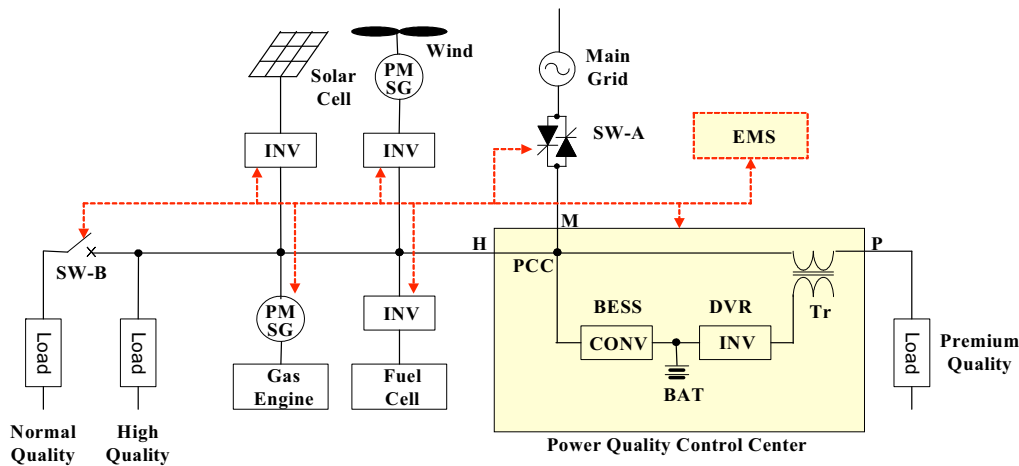


Fig. 1. Microgrid system with PQCC

Fig. 1 shows the typical power circuit of microgrid system composed of the photovoltaic power, wind power, fuel cell power, gas engine generator, PQCC, EMS and three kinds of power quality loads. As shown in Fig. 1, there are two kinds of uncontrollable power sources such as photovoltaic power and wind power. These two kind of renewable energy sources are greatly dependent on the climate conditions, which mean that the generated power of these power sources are fluctuating as time goes. In worst case the generated power can be zero. As a result, we need a power balancing device such as BESS.

Also note that we have two kinds of controllable energy sources such as the fuel cell and the gas engine. These two kinds of energy sources can generate the electricity and the heat simultaneously. Since the prices of electricity are different from each others, we need an optimum operating condition for the controllable energy sources with a help of BESS for the power balancing. Optimum operating conditions and the scheduling commands will come from the high level controller such as EMS shown in Fig. 1. In addition, we have three kinds of load levels defined as the premium quality load, the high quality load and the normal quality load. Also we have two kind of switches, SW-A and SW-B. SW-A is solid state switch which can be turned off within a half cycle of 60Hz. SW-B is the mechanical switch such as motor operated circuit breaker or magnetic contactor whose opening time is typically 2 to 3 cycles of 60Hz. SW-A is turned off when the main grid has a severe power quality problems such as severe voltage sag or interruption. The triggering level of the turning SW-A off can be controlled by an additional controller of SW-A. In any case, the premium quality load has no voltage sag problem owing to the DVR operation of PQCC. But the high quality load experience a momentary voltage disturbance during the conducting interval of thyristor switch SW-A. SW-B is turned off when there is no sufficient generation power supplied by microgrid energy sources during the isolation mode operation.

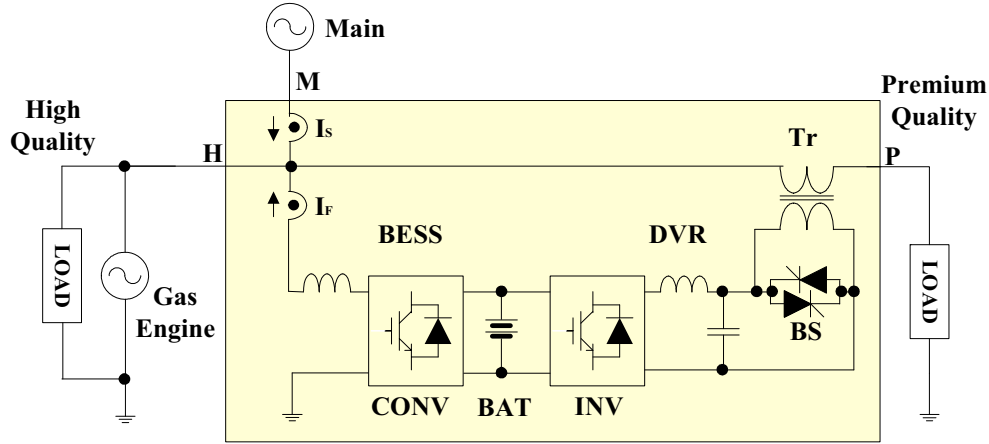


Fig. 2. Power quality control center with BESS and DVR

Fig. 2 shows the PQCC with BESS and DVR. In Fig. 2, DVR is consisted of energy storage battery, inverters, LC filters, bypass switches and an injection series transformer. During normal condition, the secondary winding of the series transformer is shorted by bypass thyristors (BS) and all switches of inverter are turned off. In order to minimize the unwanted voltage drop across the series transformer, the series transformer should have a low leakage reactance. In case of voltage disturbance, inverter is controlled to turn the bypass switches (BS) off. After all bypass switches are turned off, the inverter is controlled to compensate the voltage disturbance by injecting the controlled voltage through the series transformer with the energy stored in battery.

The control of BESS is similar to the conventional PWM converter, but it has multi-function depending on the grid conditions. During the isolation mode operation, BESS is for the stabilization of voltage fluctuation caused by the uncontrollable power source such as the photovoltaic power and the wind power. BESS can quickly respond to the sudden changes in both demand and supply of electricity that gas engine can't copy with. During grid-connected operation mode, it can be operated as APF or load leveling device with the function of battery charger. Charging and discharging command for the BESS comes from the high level EMS.

III. VOLTAGE DISTURBANCE DETECTOR AND VOLTAGE REGULATOR FOR DVR

A. Voltage Disturbance Detector for DVR

If the main utility input voltage is $V_s(t) = V_{sr} \sin(\omega t + \delta)$, then this equation can be expressed as (1) by using the trigonometric formula.

$$V_s(t) = V_{sr} \cos(\delta) \sin(\omega t) + V_{sr} \sin(\delta) \cos(\omega t) \quad (1)$$

From (1), we can know that equation is consisted of magnitude elements depending on δ and sinusoidal elements, $\sin(\omega t)$ and $\cos(\omega t)$.

Equation (1) can be expressed as (2) by applying delta rule of the neural network [3].

$$Y = WX \quad (2)$$

where Y is the estimated value by delta rule. And W and X can be expressed as (3).

$$\begin{aligned} W &= [V_{sr} \cos \delta \quad V_{sr} \sin \delta] \\ X &= [\sin(\omega t) \quad \cos(\omega t)]^T \end{aligned} \quad (3)$$

Fig. 3 shows the neural network controlled adaptive linear combiner adopting delta rule. In this special case, its output is a linear combination of its two inputs, $\sin(\omega t)$ and $\cos(\omega t)$. The components of the input vector are weighted by a set of coefficients, the weight vector W. The sum of the weighted inputs is then computed, producing a linear output, the inner product Y. The components of X may be either continuous analogue values or binary values. The weights are essentially continuously variable, and can take on negative as well as positive values. During the training process, input patterns and corresponding desired responses are presented to the linear combiner. An adaptation algorithm automatically adjusts the weights so that the output responses to the input patterns will be as close as possible to their respective desired responses. The equation of the adaptation algorithm can be written as (4).

$$W(k+1) = W(k) + \mu X(k)e(k) \quad (4)$$

where μ is the training rate.

If the training process is successful, then weighting factor (W) become the maximum value of Y. By monitoring W, we can easily obtain the magnitude (V_{sr}) of the main utility input voltage without any time delay.

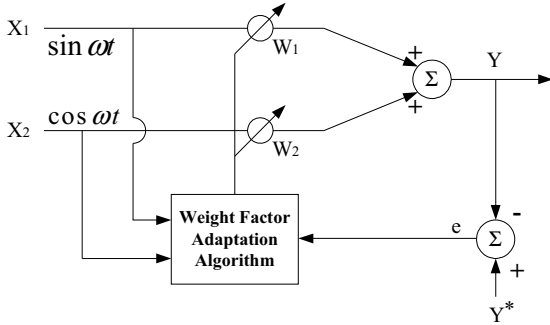


Fig.3. Neural network controlled adaptive linear combiner.

B. Voltage regulator for DVR

Fig.4 shows the control block diagram of a voltage regulator for single phase inverter. Since the controlled inverter system is not three phase inverter but single phase inverter, we can't adopt the conventional voltage regulator with three phase d-q transformation in [4-8]. As shown in Fig.4, we can obtain the q-axis component (V_{qs}) if we assume that the inverter output capacitor voltage is to be d-axis component (V_{ds}). In this case we can adopt the conventional three phase d-q transformation technique because I have both q-axis component (V_{qs}) and d-axis component (V_{ds}) from the single phase voltage. In general, q-axis variable (V_{qs}) can be obtained by using the phase shift filter. But this approach is very sensitive to the frequency variation of input voltage. In addition, phase shift filter has very poor dynamic response under the voltage transient case such as voltage sag. In this paper, we modified the conventional three phase voltage regulator to the single phase voltage regulator as shown in Fig.4.

If we assume the inverter filter capacitor voltage is d-axis variable, then q-axis variable can be defined as follows.

$$V_{ds} = V_c(t) = V_{CR} \sin \phi \quad (5)$$

$$V_{qs} = V_{CR} \cos \phi \quad (6)$$

In (5) and (6), ϕ denotes the phase shift of the capacitor voltage to the utility input voltage $V_s(t)$. From the control block diagram of Fig. 4, we can obtain (7) and (8).

$$V_{de} = V_{CR} \sin \phi \sin \theta + V_{CR} \cos \phi \cos \theta \quad (7)$$

$$V_{qe} = V_{CR} \cos \phi \sin \theta - V_{CR} \sin \phi \cos \theta \quad (8)$$

If the inverter output capacitor voltage is well regulated, then we can assume that $V_{CR} = V_{ref}$ and $\phi = \theta$. We can obtain (9) and (10) by using (7) and (8).

$$V_{de} = V_{ref} \quad (9)$$

$$V_{qe} = 0 \quad (10)$$

As a result, we can assume that the q-axis variable is as follows.

$$V_{qs} = V_{ref} \cos \theta \quad (11)$$

$$V_{ref} = V_{SR} - V_{LR}^* \quad (12)$$

However relationships (9) and (10) can be applied under ideal condition, but in reality we need an additional compensation for the time delay of inverter LC filter and dead time effects of inverter switches. To compensate the non-ideal effects, we adopted a PI and a feed-forward control concept (V_{de} , V_{qe} terms) as shown in Fig.4. It can be shown in Fig.4 that we are only using the output of d-axis controller to the PWM signal since the magnitude (V_{qe}) is well controlled to be zero. Note that we can obtain the q-axis variable (V_{qs}) from (11) only by using voltage reference (V_{ref}) and phase tracking information ($\cos \theta$).

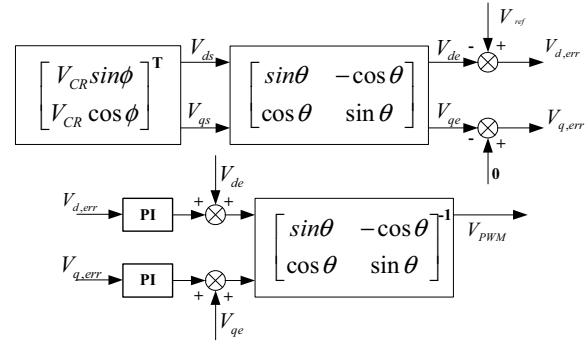


Fig. 4. Control block diagram of voltage regulator for single phase inverter

IV. CURRENT CONTROLLER FOR BESS

Fig. 5 shows the power block diagram of BESS, which is similar to the APF except for the battery in DC side. Fig. 6 shows the control block diagram for BESS, where load current (I_L) is obtained by adding the source current (I_S) and the filter current (I_F). The controller of BESS is similar to the controller of APF [9-11], except for the DC link voltage controller for the charging of battery. In Fig. 6, the instantaneous power is calculated by using the line voltage and the load current with a help of park's vector [9]. After removing the fundamental component (DC component) from the instantaneous power, we can only obtain the harmonic component of the load current. By using the hysteresis current controller, we can compensate the harmonic component of the load current. Concerned to the battery charging operation, we can control the DC link voltage by controlling the p-component of the instantaneous power as shown in Fig. 6. Voltage reference comes from high level controller EMS.

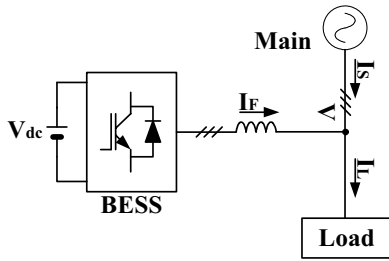


Fig. 5. Power block diagram for BESS

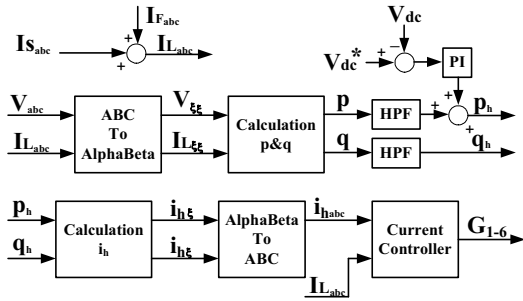


Fig. 6. Control block diagram for BESS

V. SIMULATION RESULTS FOR PQCC

In order to analyze the operational characteristics of PQCC by using proposed voltage disturbance detection method, output voltage regulator and BESS control, computer simulation was performed by using the parameters in table I.

Fig. 7 shows the simulation results of the proposed voltage disturbance detector. In Fig. 3, unbalanced sag voltage is applied to the new voltage disturbance detector. Note that only phase-A voltage has sag, but other two phase voltages are normal. Fig. 7b shows that neural network controlled method has no ac component, and no time delay to determine the voltage disturbance instance. Fig.7b shows that we can quickly obtain the amplitude of the input voltage when there is voltage disturbance in the source voltage.

Another merit of the neural network controlled method is that it can track the amplitude of each phase voltage independently. If we know that only one or two phase voltages have a disturbance, then we can control only the corresponding phase voltages. On the other hand, it is very difficult to identify and to control the corresponding phases independently when we adopt the conventional three phase d-q transformation method.

Fig. 8 shows the source voltage, load voltage and injection voltage during sag operation. From Fig. 8, we can see that DVR is operating well to maintain the load voltage to be constant during sag interval by detecting the voltage disturbance and compensating it.

Fig.9 shows the control characteristics of output voltage regulator. As shown in Fig. 9, q-axis variable is leading d-axis variable by 90° as expected. Also V_{de} and V_{qe} are well tracking the reference signal V_{de}^* and V_{qe}^* . As

a result, the load voltage of DVR is well compensated under the voltage sag conditions.

Table I. Parameters for PQCC simulation

Source	440V, 60Hz	
Load	1000kVA	
APF	Filter L_f	100uH
DVR	DC Link Voltage	600V
	Switching frequency	2kHz
	Filter L	200uH
	Filter C	800uF
	Injection Tr.	480V:127V

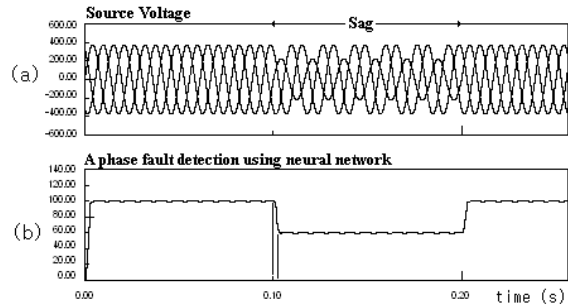


Fig. 7. Simulation result for voltage disturbance detection

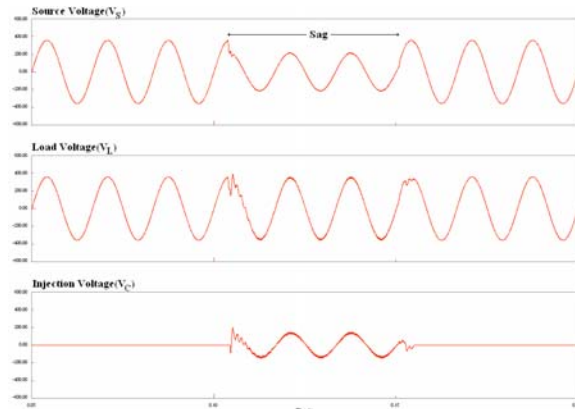


Fig. 8. Simulation result for voltage sag compensation

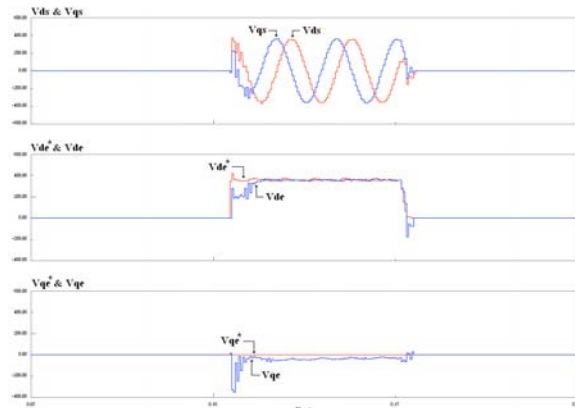


Fig. 9. Simulation results for the operation of voltage regulator

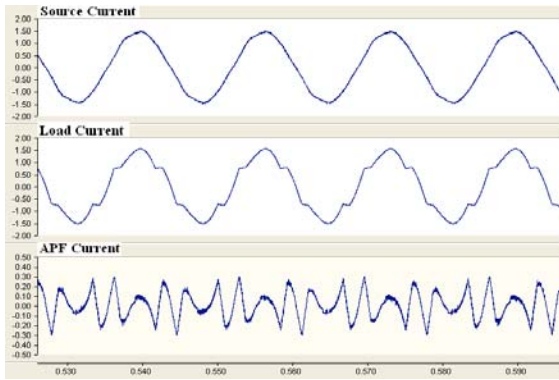


Fig. 10. Simulation result for harmonic current compensation

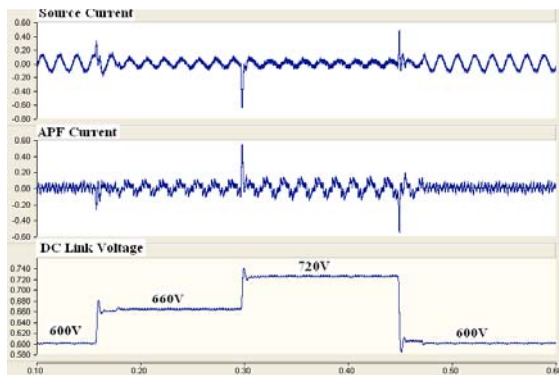


Fig. 11. Simulation result for battery charging

Fig. 10 shows the simulation results for harmonic current compensation. Load current is summation of the resistive current and the phase controlled rectifier input current. As shown in Fig.10, the source current waveform is nearly sinusoidal.

Fig. 11 shows the simulation results for the battery charging operation. The rated DC battery voltage is 600V, and the floating charging voltage is 660V and the equalizing charging voltage is 720V. As shown in Fig. 11, the DC link voltage is well tracking the reference voltage.

CONCLUSIONS

This paper describes the PQCC for the microgrid system. Even though PQCC can do many kinds of functions, we only discussed the DVR and APF operations in grid-connected operation mode. In this paper we proposed the new voltage disturbance detection method using the neural network for the control of DVR. The proposed disturbance detection method shows the minimum time delay to determine the disturbance instance. Also new voltage regulator for single phase inverter was proposed by modifying the conventional three phase d-q transformation technique. Proposed voltage disturbance detection method and the new voltage were verified through the computer simulation. Finally APF operation with BESS was verified with the function of battery charger. In our next works, we will discuss the

voltage stabilization in isolation operation mode with considering the effects of photovoltaic power, the wind power, fuel cell power and gas engine generation.

ACKNOWLEDGMENT

This work was supported in part by the Korea Ministry of Knowledge Economy under the project of “Development of standard and modular based devices for microgrid system.”

REFERENCES

- [1] C. Marnay and R. Firestone, “Micro grids: An Emerging paradigm for meeting building electricity and heat requirements efficiently and with appropriate energy quality”, European Council for an Energy Efficient Economy 2007 Summer Study, 2007.
- [2] Y. Fujioka, H. Maejima and et. al, “Regional Power Grid with Renewables Energy Resources: A demonstration Project in hachinohe”, 2006 CIGRE Session, C6-305, 2006.
- [3] B. Widrow and M. A. Lehr, “30 Years of Adaptive Neural Networks : Perception, Madaline, and Back Propagation”, *Proceeding of The IEEE*, Vol. 78, No. 9, September, 1990, pp1415-1442
- [4] A. Ghosh and G.Ledwich, “Compensation of Distribution System Voltage Using Dynamic Voltahe Restorer”, *IEEE Tran. on Power Delivery*, Vol. 17, No. 4, Oct, 2002, 1030-1036
- [5] J.G. Nielsen and F. Blaabjerg, “A Detailed Comparison of System Topologies for Dynamic Voltage Restorer”, *IEEE Tran. on Industry Application*, Vol. 41, No.5, Sept 2005, pp 1272-1280
- [6] C. Fitzer, M. Barnes and P. Green, “Voltage Sag Detection Technique for a Dynamic Voltage Restorer”, *IEEE Tran. on Industry Applications*, Vol. 40, No. 1, Jan, 2004, pp203-212
- [7] P.T. Cheng, C.C. Huang, C.C. Pan, S. Bhattacharya, “Design and Implementation of Series Voltage Sag Compensator under Practical Utility Conditions”, *IEEE Tran. on Industry Applications*, Vol. 39, No. 3, May, 2003, pp844 - 853
- [8] J.G. Nielsen, M. Newman, H. Nielsen and F. Blaabjerg, “Control and Testing of a Dynamic Voltage Restorer at Medium Voltage Level”, *IEEE Tran. On Power Electronics*, Vol. 19, No.3, May, 2004, pp 806-813
- [9] H. Akagi, H. Fujita, “A New Power Line Conditional for Harmonic Compensation in Power Systems”, *IEEE Trans. Power Delivery*, Vol. 10, No. 3, 1995, pp1570-1575.
- [10] M.T. Tsai, C.E. Lin, W.I. Tsai and C.L. Huang, “Design and Implementation of Demand-side Multifunction Battery Energy Storage System”, *IEEE Tran. on IA*, Vol 42, No.6, 1995, pp 642-652
- [11] S.J. Chiang, S.C. Huang and C.M. Liaw, “Three-phase Multi-Functional Battery Energy Storage System”, *EPE, IEE Proceedings Vol 142, Issue 4, 1995, pp275-284*